ISSN 0965-545X, Polymer Science, Ser. A, 2014, Vol. 56, No. 6, pp. 928–935. © Pleiades Publishing, Ltd., 2014.

THEORY AND SIMULATION

A Multiscale Simulation Model for Poly(ethylene oxide)[1]

Visit Vao-Soongnern

Laboratory of Computational and Applied Polymer Science (LCAPS), School of Chemistry, Institute of Science, Suranaree University of Technology, Nakhon Ratchasima 30000, Thailand

e-mail: visit@sut.ac.th

Received February 12, 2014;
Revised Manuscript Received July 2, 2014

Abstract—An overview of the recent development of a multiscale simulation of amorphous polymeric materials at the bulk density is presented. Poly(ethylene oxide), (PEO), (CH_3O–[CH_2–CH_2–O]$_n$$CH_3$) was selected to illustrate the method. The model starts from an ab initio quantum chemistry to obtain the statistical weights of polymer conformation based on the rotational isomeric state (RIS) theory. PEO chains were then mapped to a coarse-grained model using the modified RIS model onto the second nearest neighbor diamond (2*nnd*) lattice. The average non-bonded interactions were treated by the discretized Lennard-Jones (LJ) potential. Bulk PEO melts with molecular weight up to 8000 g/mol was generated and equilibrated. The on-lattice properties such as molecular size and conformational statistics agree well with the theory. Fully atomistic amorphous PEO models can be obtained by the reverse-mapping procedure to recover the missing atoms. After an energy minimization step, properties including torsional angle distribution, solubility parameter and static neutron scattering structure factor are in good agreement with experimental results.

DOI: 10.1134/S0965545X14060121

INTRODUCTION

In 2013, the Nobel Prize in chemistry was awarded jointly to Martin Karplus, Michael Levitt and Arieh Warshel "*for the development of multiscale models for complex chemical systems*." This review is motivated by them to apply a similar concept of the multiscale model for an investigation of amorphous polymeric materials. Polymers are complex macromolecules that display structure ranging from the Angstrom level of the individual backbone bond to the scale of the radius of gyration, which can reach ten of nanometers. The time scales of the dynamic processes span an even wider range, from femtoseconds to milliseconds, seconds to hours in glassy materials or even larger [1]. For example, the time that a polymer chain in a melt needs to lose memory of its initial conformation is around $N^2 \times 10^{-11}$ s for unentangled melts [2, 3] and around $(N^3/N_e) \times 10^{-11}$ s for entangled melts [3, 4], where N is the degree of polymerization of the polymer, N_e and is the chain length between entanglements.

No single model or simulation algorithm can cover this range of length and time scales. Therefore, molecular and coarse-grained models for polymeric materials range from those including quantum effects and electronic degree of freedom; to chemically realistic, classical model; to coarse-grained or even mesoscale models that retain only the most essential elements of the polymer system to be simulated. One of the most important problems in computational materials research, which holds particular challenges for polymer materials, is multiscale simulation-the bridging of length and time scales and the linking of computational methods to predict macroscopic properties and behavior from fundamental molecular processes [5].

In 1995, a Monte Carlo (MC) simulation technique that employed the modified RIS models of the coarse-grained chains mapped onto the second nearest neighbor diamond (2*nnd*) lattice at the bulk density was developed [6]. Since then, several examples of this MC simulation have been performed during the past years [7–27]. The MC simulation on 2*nnd* lattice offers an advantage by discretizing the phase space and utilizing fast integer algorithms. This technique consists of three steps: (i) mapping of an atomistic system onto a coarse-grained representation on a sparsely occupied high coordination lattice, (ii) performing MC simulations on the high coordination lattice, and (iii) reverse mapping of selected snapshots from the high coordination lattice back to an atomistic system.

In this work, we have added one more step to this MC technique by incorporating the quantum chemistry calculation to obtain more accurate description of the conformational characteristics of polymer chain. Poly(ethylene oxide), PEO, was selected as a system to illustrate the concept of this multiscale technique. PEO, –[CH_2–CH_2–O]$_n$–, is one of the simplest polymer structures but its conformational characteristics are very interesting from the theoretical description. The spatial configuration of a single PEO chain was first treated theoretically within the framework of the Rotational Isomeric State (RIS) model [28, 29]. There is still an ambiguous assignment of numerical values to

[1] The article is published in the original.

statistical weights that has not been achieved for the chain occurring under various conditions. The anomaly associated with the *gauche* preference around the OC–CO bond has been pointed out on the basis of a comparison of the calculated and experimental results on the conformational dependent properties. Various RIS parameter sets are reported in literatures that reproduce the same conformational characteristics of PEO [30].

There are quite number of past studies for simulation of multi-chain PEOs; for example, system of atomistically detailed models at bulk density employed either short PEO chains [31, 32]. The restriction for large systems in those previous studies was imposed by the difficulty in thoroughly equilibrating the dense models when they are expressed at fully atomistic details. These larger systems should be tractable for simulation when the models are expressed with coarse-grained RIS chains that retain contact with reality, and allow reverse mapping back to atomistically detailed models.

Previous investigation using this MC simulation on 2*nnd* lattice includes homogeneous polymers and their mixtures such as polyethylene, polypropylene, polyvinylchloride and polystyrene [7–27]. For PEO system, the simulation was applied successfully to study the dependence of threading of small cyclic poly(ethylene oxide) molecules by linear poly(ethylene oxide) chains in the melt. The system size were 21 beads on the lattice equally to 42 backbone atoms, $CH_3(OCH_2–CH_2)_{13}OCH_3$ and 42–crown–14 for the linear and cyclic molecules, respectively [19]. The equilibration of the degree of threading in this polymer system was impossible with the currently available computer resources when an atomistically detailed model was used. By this MC technique, the system was equilibrated relatively quickly, allowing for the equilibrium properties to be evaluated. In addition, we recently studied the conformation and diffusion of larger cyclic and linear poly(ethylene oxide), PEO, blends for the length from 50 to 200 repeating units. The main focus was to validate the simulation method for the specific polymer with a comparison to the prediction from theory for relatively long chain length regime [27].

In this report, a systematic and complete illustration is presented for this method as presented below.

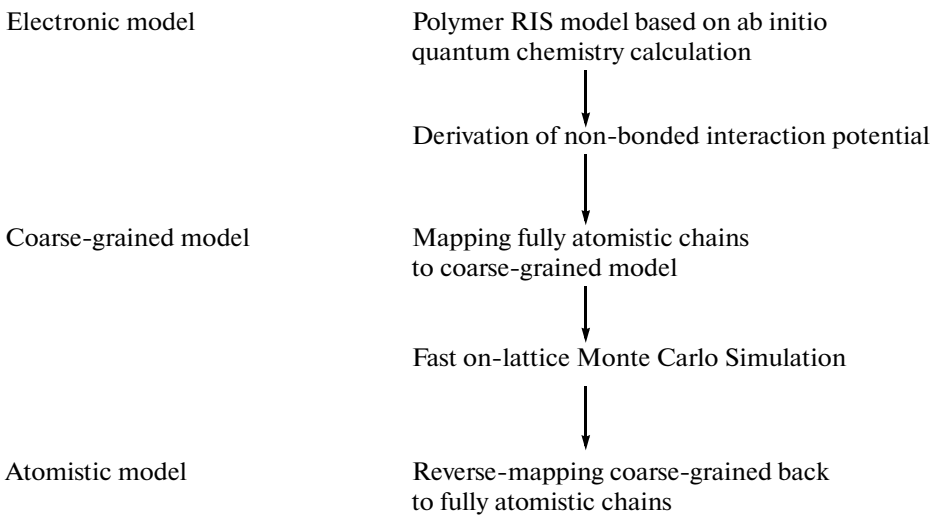

The outline of this multiscale simulation starts from an electronic structure calculation of a model compound that represents the local conformational characteristics of PEO. The modified RIS model for coarse-grained PEO chains and the discretized version of non-bonded energy are incorporated with the mapping procedure on 2*nnd* lattice which represent the short- and long-range interaction of the simulation model at the bulk density. A fast Metropolis Monte Carlo (MC) algorithm is employed to equilibrate the bulk structure. Finally, the results from the on-lattice simulation and from the fully atomistic model after the reverse-mapping procedure are presented and compared with experiment.

METHOD

Model

Monte Carlo technique was performed on a coarse-grained PEO chains that were mapped onto the second nearest diamond (2*nnd*) lattice [6]. Each occupied site contains either $–CH_2–CH_2$ or $–CH_2–O$ unit, connected by coarse-grained bonds of length 2.39 Å. Every bead was treated identically. The melt density of PEO was simulated at 373 K close to the temperature used in the molecular dynamic simulation and neutron scattering experiment [31, 32]. The lattice has occupancy only about 20%. The torsional angles are restricted to *trans* and two *gauche* states. The fully ato-

mistic system can be recovered at any time during the simulation.

Energies

The RIS model for poly(A–A–B) chains with A = CH_2 and B = O, in which all bonds are subject to a symmetric 3-fold torsion potential with the nearest neighbor interdependence, is given by the following statistical weight matrices for successive bonds of A–A, A–B, and B–A [28].

$$U_{AA} = \begin{bmatrix} 1 & \sigma_{BB} & \sigma_{BB} \\ 1 & \sigma_{BB} & \sigma_{BB}\omega_{AB} \\ 1 & \sigma_{BB}\omega_{AB} & \sigma_{BB} \end{bmatrix} U_{AB}$$

$$= \begin{bmatrix} 1 & \sigma_{AA} & \sigma_{AA} \\ 1 & \sigma_{AA} & \sigma_{AA}\omega_{AB} \\ 1 & \sigma_{AA}\omega_{AB} & \sigma_{AA} \end{bmatrix} U_{BA} = \begin{bmatrix} 1 & \sigma_{AA} & \sigma_{AA} \\ 1 & \sigma_{AA} & \sigma_{AA}\omega_{AA} \\ 1 & \sigma_{AA}\omega_{AA} & \sigma_{AA} \end{bmatrix} \quad (1)$$

In the matrices, the rows and columns define the states of bonds $i - 1$ and i, respectively. The three accessible rotational isomeric states for each bond are t, g^+, and g^-, used in this order in the matrices. The σ_{CC} and σ_{CO} are the statistical weights for the C···C and C···O type first-order interactions, which result from the rotational degree of freedom of the middle bond in a three-bond unit, and ω_{CO} and ω_{CC} represent the O–C or C–C and C–O type second-order interactions, respectively, for $g^{\pm}g^{\mp}$ state in the middle of a four-bond unit with two rotational degrees of freedom.

Table 1 gives the mapping between the rotational isomer pairs for two successive bonds on the diamond lattice and the length of the segment connecting beads i and $i + 2$ on the 2*nnd* lattice. The states are grouped together and their statistical weights are averaged in order to obtain a 4×4 matrix, where the rows and columns represent the four states of the segments connecting beads (i and $i + 2$) and ($i + 1$ and $i + 3$). Geometric averaging of statistical weights of indistinguishable states leads to the following coarse-grained statistical weight matrix, with $\sigma = (\sigma_1\sigma_2)^{1/2}$, $\omega_1 = \omega_{CO}$ and $\omega_2 = \omega_{CC}$.

$$U^G_{2nnd} = \begin{bmatrix} 1 & 4\sigma & 2\sigma^2 & 2\sigma^2\omega_2 \\ 1 & 4\sigma\omega_1^{1/8} & 2\sigma^2\omega_1^{1/4} & 2\sigma^2\omega_1^{1/4}\omega_2 \\ 1 & 4\sigma\omega_1^{1/4} & 2\sigma^2\omega_1^{1/2} & 2\sigma^2\omega_1^{1/2}\omega_2 \\ 1 & 4\sigma\omega_1^{1/4} & 2\sigma^2\omega_1^{1/2} & 2\sigma^2\omega_1^{1/2}\omega_2 \end{bmatrix} \quad (2)$$

This 4×4 matric can be further reduced in dimensions to 3×3, by suitable combination of the last two rows and columns.

Table 1. Four states include the conformations on diamond lattice and lengths of segment connecting bead i and $i + 2$ on the 2*nnd* lattice

State on 2*nnd* lattice	Conformations on diamond lattice	Lengths of segment connecting bead i and $i + 2$ on the 2*nnd* lattice[a]
A	*tt*	4.80
B	tg^+, tg^-, g^+t, g^-t	4.15
C	g^+g^+, g^-g^-	3.40
D	g^+g^-, g^+g^-	2.40

[a] The average bond length for PEO is closer to 1.47 Å.

Table 2. RIS model of PEO from ab initio calculation of DME model compound

Conformer	RIS representation	Ab initio energy[a], kcal/mol	RIS energy[b]
ttt	0	0.00	0.0
tgt	σ_{OO}	0.14	0.1
ttg	σ_{CC}	1.43	1.4
tgg	$\sigma_{OO} + \sigma_{CO}$	1.51	1.5
tgg'	$\sigma_{OO} + \sigma_{CO} + \omega_{CO}$	0.23	0.2
gtg	$2\sigma_{CC}$	3.13	2.8
gtg'	$2\sigma_{CC}$	3.08	2.8
ggg'	$\sigma_{OO} + 2\sigma_{CC} + \omega_{CO}$	1.86	1.6
g'gg'	$\sigma_{OO} + 2\sigma_{CC} + 2\omega_{CO}$	2.41	0.3
ggg	$\sigma_{OO} + 2\sigma_{CC}$	1.64	2.9

[a] The calculation was performed at MP2/6-311+G*.
[b] Parameter set are $E_{OO} = 0.1$, $E_{CC} = 1.4$ and $E_{CO} = -1.3$ kcal/mol.

RIS Parameters from Electronic Structure Calculation

Various RIS models have been proposed to calculate the conformational dependent properties of a single PEO chain [30]. The major difference among the conformational energy parameter sets proposed are found in the assignment of the so-called second-order interaction energy between two oxygen atoms (E_ω), ranging from 0.6 to −1.7 kcal/mol, and to some extent, in the *gauche* energy (E_σ) relative to the *trans* state. Due to strong repulsion, the second-order interaction energy between two methylene group atoms (E_ψ) is very high and the statistical weight can be set as: $\omega_{CC} = 0$. In this work, the RIS parameters for PEO can be determined using quantum chemistry calculation. A small molecule, 1,2-dimethoxylethane (CH_3–O–CH_2–CH_2–O–CH_3; DME), was selected as a representative model of PEO. To find the low energy conformation, a semi-empirical (AM1) method [33] was adopted with the search algorithm provided by HyperChem7 software. The conformational energies were obtained by rotating the dihedral angles and the

optimized structure should be corresponded to the energy minimum structure for each pair of dihedral angles. An increment of dihedral angles (ϕ_i, ϕ_j) was set to 20° (rotation from 0° to 360°) according to each skeleton bond as: O–C, C–C and C–O bond, respectively. Next, geometries and conformational energies of the selected low energy conformation of nine rotamers of DME compound were optimized at the HF/6-311 + G^* level using Gaussian software package. The energies for electron correlation effect for each conformer were estimated by MP2 calculation with the same basis set [33]. The energy of *gauche* conformation of the O–C–C–O bond relative to the *trans* conformation depends strongly not only on the basis set size but also on electron correlation effects. Statistical weights (Boltzmann populations) of each conformer are readily calculated based on the relative electronic energy and degeneracy of each conformation. This ab initio calculation yield energetics relative to the *ttt* conformer and the *tgg* and *tgg*' energies relative to *tgt* energies. The *tgg*' state is much more favorable and thereby accounting for the prediction of a relatively high population of *tgg* + *tgg*' state. The *tgg*' conformer appears to be the result of strong attractive interactions between an O atom and a hydrogen on the opposite methyl group. The second-order model takes into account interactions between atoms or groups separated by a maximum of four bonds and hence two consecutive torsions. Using values of $E_{OO} = 0.1$, $E_{CC} = 1.4$, and $E_{CO} = -1.3$ kcal/mol, for example, one can represent the energies of eight of the ten DME conformers, including *tgg*' reasonably well as indicated in Table 2.

Long-Range Interaction

The long-range interactions are obtained from a discretized form of the Lennard-Jones (LJ) potential, in which the second virial coefficient (B_2) for polymers is evaluated similar to a non-ideal gas using the Mayer f function according to the imperfect gas theory as follows [7]:

$$B_2 = \frac{1}{2}\int\{\exp[-\beta u(r)] - 1\}\,dr = \frac{1}{2}\int f dr, \qquad (3)$$

where $\beta = 1/kT$, f is the Mayer function and $u(r)$ is the inter-particle LJ potential of the form

$$u = \begin{cases} \infty & r < 2.4\ \text{Å} \\ u_{LJ} = 4\varepsilon\left[\left(\dfrac{\sigma}{r}\right)^{12} - \left(\dfrac{\sigma}{r}\right)^{6}\right] & r > 2.4\ \text{Å} \end{cases} \qquad (4)$$

where ε and σ are known as the well depth and the collision diameter, respectively. On the 2*nnd* lattice, the prohibition of double occupancy of any site implies $u = \infty$, $r < 2.4$ Å, and u at the remaining sites can be represented by a truncated Lennard-Jones potential energy function. r is the spacing between two interacting beads. On the lattice, B_2 is written in a discretized form by separating the integral into the sub-integral for each lattice cell and regrouping them for each neighbor. The σ value is obtained by first noting that σ for propane is within 1% of $(3/2)^{1/3}\sigma_{\text{ethane}}$. Therefore, the required value of σ for a coarse-grained bead of PEO can be estimated from the data for methyl ether (CH_3OCH_3, σ = 4.307 Å) as

$$\sigma_{PEO} = (2/3)^{1/3}\sigma_{\text{methylether}} \qquad (5)$$

from which $\sigma_{PEO} = 3.76$ Å. The ε for two backbone atoms of PEO were estimated by fitting the experimental bulk density of PEO a series of simulations of free-standing PEO thin films that have different ε values. With this method, LJ parameters at the simulated temperature 373 K are: $\sigma_{PEO} = 3.76$ Å and $\varepsilon/k_B = 154$ K. Discretization of this LJ potential produces the long-range interaction energies. For example, the parameters for the first five shell of PEO at 373 K are 8.113, –0.213, –0.339, –0.067 and –0.017 kJ/mol. The first shell is highly repulsive while the interaction parameter for the second neighbor shell is negative. This interaction parameter covers the distance 2.4–4.8 Å, which includes the collision diameter, 3.76 Å. Therefore, the attractions are dominated in the second neighbor shell. Only the first three shells are applied. These parameters yield a cohesive structure with bulk density that most closely matches the experimental density of 1.06 g/cm^3 [19].

Moves

Single bead and pivot move were used in order to improve the simulation efficiency. In a pivot move, bond vectors for a subchain of the original conformation were reversed to create a new configuration [13]. A subchain with two to six beads was applied for pivot moves. The moves are accepted or rejected according to the Metropolis criterion [34]:

$$P_{\text{move}} = \min[1, P_{\text{new}}/P_{\text{old}}], \qquad (6)$$

where P_{new} and P_{old} are the probabilities of the configurations before and after the move made, respectively. The moves are accepted if they are generating a lower energy configuration. Otherwise, a move is accepted with the probability of $P_{\text{new}}/P_{\text{old}}$ i.e. with Boltzmann factor representing the degree of increase in the conformation energy. The Metropolis criteria were applied to determine the move. For every Monte Carlo step (MCS), single bead moves and multiple bead pivot moves were performed randomly. Every bead was tried once in both single bead moves and pivot moves.

System Description

The simulations were performed in a periodic box with 20 unit lengths on each side of the lattice; i.e., $L_x = L_y = L_z = 20$ which is equivalent to 47.8 Å. For all

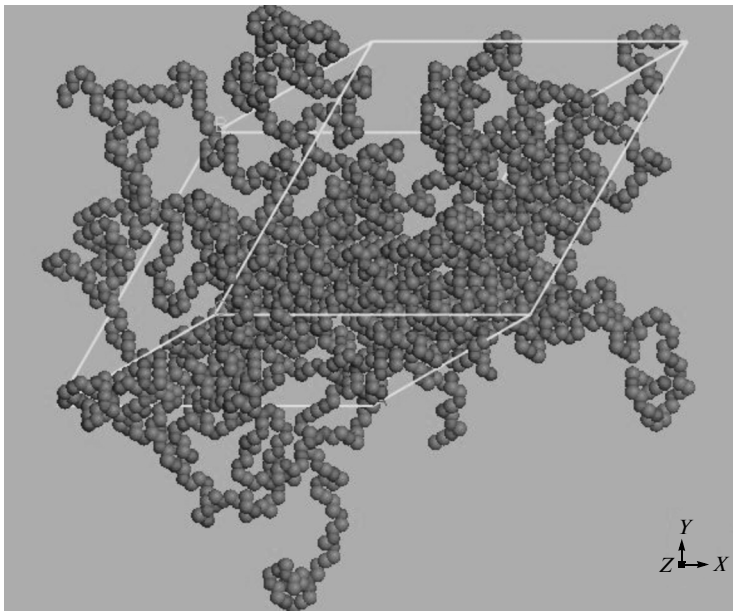

Fig. 1. Specific snapshot from the Monte Carlo simulation on the 2*nnd* lattice (10 chains of $CH_3(OCH_2CH_2)_{111}OCH_3$ at 373 K.

systems, a total of 1680 beads are put into this box to achieve the experimental density for PEO at 373 K. The size of the system is 10 chains of $N = 168$. Each chain can be reverse-mapped into 336 backbone atoms, $CH_3(OCH_2CH_2)_{111}OCH_3$. The initial configuration was randomly distributed in the periodic box. A sufficiently long simulation is run until the system achieves equilibrium. After equilibration, an additional 10 million MCS are performed and recorded every 10000 MCS.

Energy Minimization (EM) of Reverse-Mapped Snapshots

The coordinates of the carbon, oxygen and hydrogen atoms in the chains that have been reverse mapped back onto the tetrahedral lattice were created. EM of the bulk snapshot was performed by Discover module in Material Studio software with PCFF force field until the gradient is less than 0.1 kcal/(mol Å). The three stages of the EM procedure are summarized as: (1) Non-bonded potentials are scaled by 10^{-5} to avoid large conformational changes due to the initial close contacts among the hydrogen atoms. The process is performed until the gradient is less than 10 kcal/(mol Å). (2) Non-bonded potential scaling is reduced by a factor of 10, in four successive stages, to 10^{-1}. At each stage, the minimization is carried out till the gradient is less than 10 kcal/(mol Å). (3) Finally, non-bonded potential scaling is reduced to 1, i.e., no scaling. The state is performed till the gradient is less than 0.1 kcal/(mol Å). In all steps, the steepest descents method is used if the gradient is greater than 1000 kcal/(mol Å), and the conjugate gradient is used otherwise. Figure 1 shows the specific snapshot from the fully atomistic reverse-mapped structure.

RESULTS AND DISCUSSION

Equilibration

Equilibration of the systems can be determined by evaluating the orientation autocorrelation functions (OACFS) defined using the end-to-end vector of the linear chain, $\langle \vec{R}(t) \cdot \vec{R}(0) \rangle$. From Fig. 2, the equilibrium condition is satisfied within 10 million MCS.

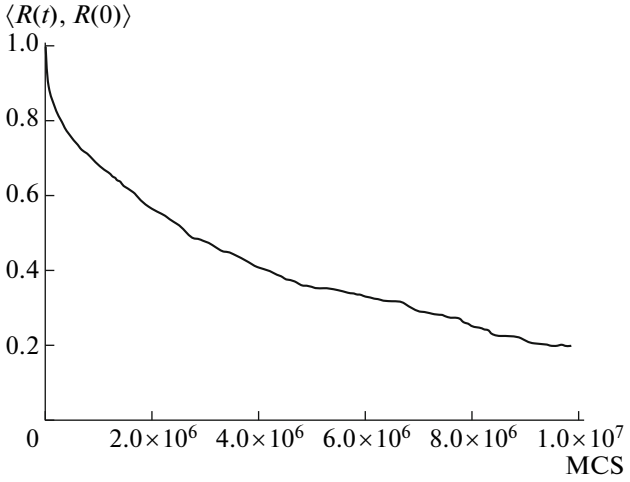

Fig. 2. Orientation autocorrelation function (OACF) of the end-to-end vectors of the PEO chains.

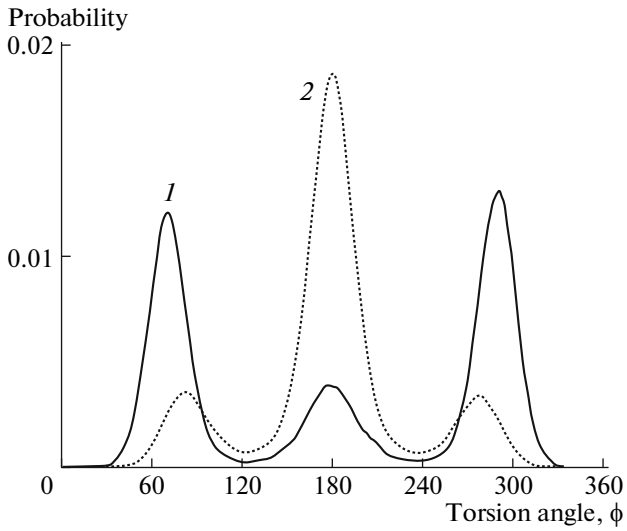

Fig. 3. Distribution of the torsion angles in a representative snapshot along the (*1*) CO–OC and (*2*) CO–CC backbone atom sequence for PEO after reverse mapping and subsequent EM.

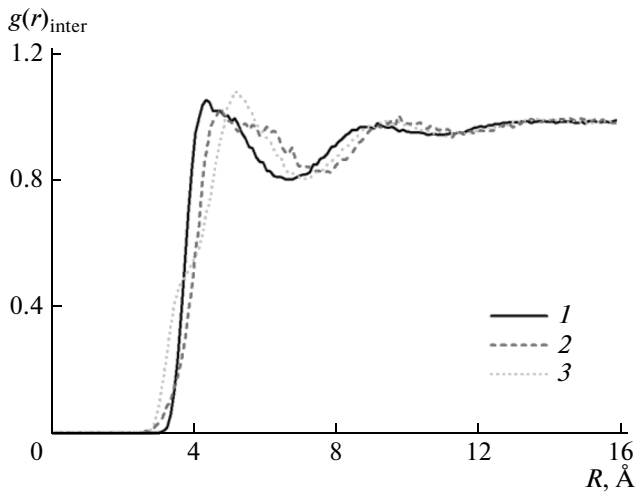

Fig. 4. Intermolecular (*1*) C–C, (*2*) O–O and (*3*) C–O pair distribution for amorphous PEO melts as a function of separation distance after MC/EM equilibration and minimization.

Chain Dimensions

Initial guess structures from the simulation gave the characteristic ratio, $C_n = \langle R^2\rangle/nl^2$, ($\langle R^2\rangle$ is the mean square end–to–end distance, l is the bond length and n is number of bonds), and the radius of gyration for chain with $N = 168$ as $C_n = 3.7 \pm 1.4$, $\langle R^2\rangle^{1/2} = 53.33 \pm 8.14$ Å and $\langle R_g^2\rangle^{1/2} = 21.89 \pm 2.58$ Å. These values are comparatively closed to the ones calculated from the RIS model of PEO chains with similar geometries. During an EM, after the reverse-mapping, the overall shape of PEO chains did not change much. The dimensions are practically the same for the minimized structures as for the initial guesses e.g. $\langle R_g^2\rangle^{1/2} = 20.43 \pm 5.36$ Å. The simulation ratio of $\langle R\rangle/\langle R_g\rangle$ is 5.998 which is closed to the theoretical Gaussian behavior where $\langle\langle R\rangle/\langle R_g\rangle$ is 6 for sufficient long chain [28]. The slope of $\log(N)$ vs. $\log\langle R_g\rangle$ line is calculated as 1.01 ± 0.02. Thus it can be concluded that the universal scaling law is satisfied reasonably well when the chain are sufficiently long (M_w is about 4000 g/mol). The distribution width of $\langle R_g\rangle$ can be determined by calculating the ratio $\langle R_g^4\rangle/\langle R_g\rangle^2$. This ratio from our simulation was 1.24 ± 0.20 which is close to 19/15 for the long Gaussian chain. Also, the dimensionless ratio $\langle R\rangle/\langle R\rangle$ approached the Gaussian limit of 5/3 with increasing N [28].

Distribution of Torsion Angles

After reverse mapping, but before minimization, the distribution of torsion angles is limited to the three values, about 180° and ±60°, that are allowed on the tetrahedral lattice. During the EM, the torsion system moves off-lattice, and the δ functions at 180° and ±60° are replaced by continuous distributions. The heights of the δ functions were 0.28(0.66) at 180°, and 0.36 (0.17) at ±60° for OC–CO and CC–OC torsional angle, respectively. As shown in Fig. 3, the continuous distribution produced by EM maintains the strong preference for torsion angles near 180° and ±60°. The population of the *t* state is 0.28 and 0.66 for the CO–CC and OC–CO, respectively. The oxygen *gauche* effect is clearly seen in the OC–CO conformer population. The remaining population is nearly equally distributed between the two *g* states. The RIS model employed in the mapping procedure predicts 64.4% of the bonds are in *t* states.

Cohesive Energy Density and Solubility Parameters

The cohesive energy, U_{coh}, is the energy associated with the intermolecular interactions only and can be estimated by taking the difference between the total energy of the microstructure, U_{tot}, and that of the isolated parent chain, U_{par}. Hildebrand's solubility parameter, δ, is the square root of the cohesive energy density according to the equation

$$\delta = (CED)^{1/2} = \left[\frac{\Delta E_v}{V_1}\right], \qquad (7)$$

where ΔE_v is the molar energy of vaporization and V_1 is the molar volume of liquid. The CED of reverse-mapped and energy-minimized snapshots was calculated. The experimental Hildebrand solubility parameter of PEO is reported to be $9.9 \pm 1 \text{cal}^{1/2}/\text{cm}^{3/2}$ at room temperature. The value of reverse-mapped and

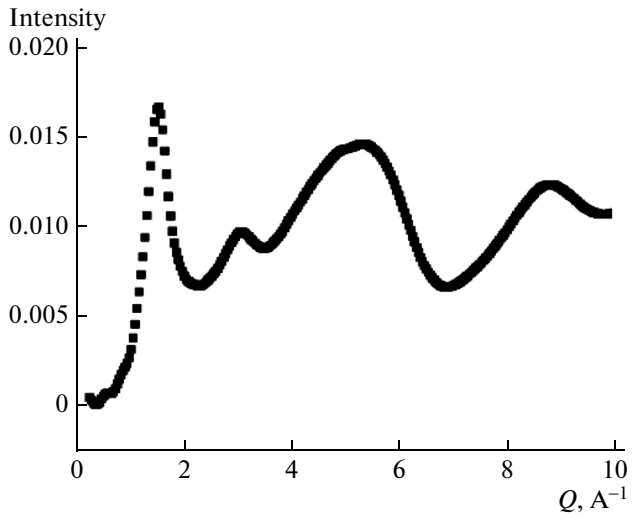

Fig. 5. Static normalized coherent structure factor $I(Q)$ from neutron diffraction experiment of fully atomistic PEO model after a reverse-mapping and EM. Three peaks at $Q = 0.58$, 1.53 and 3.07 $Å^{-1}$ are consistent with experimental results (PEO melts at 363 K) at: $Q = 0.6$, 1.3 and at 3.0 $Å^{-1}$.

EM snapshots ($\delta = 9.74$ $cal^{1/2}/cm^{3/2}$) are close to the experimental range [35].

Positional Order

The pair correlation function for three different pairs of elements (C···C, C···O and O···O) were calculated as presented in Fig. 4. The first peak in these pair distribution functions occurs between 4 and 5 Å and is indicative of nearest-neighbor chain packing. The distance is less than that seen for the first peak in the C–C pair distribution function in normal alkane [16]. The closer chain packing in PEO reflects the greater density of the PEO systems. From the elemental pair distribution functions, it is straightforward to extract scattering patterns. The direct comparison of theoretical against experimental results constitutes a useful check for the structural predictions of the model.

Neutron scattering has proven to be very useful in determining structure of polymer melt to help illuminate the packing of polymer chains in amorphous phase. The neutron elastic structure factor $S(Q)$ was calculated as a function of scattering vector magnitude $Q = (4\pi/\lambda)\sin(\theta)$, where 2θ is the scattering angle and λ is the wavelength of scattered radiation. The method was using the formulation previously employed by Ludovice [36] and implemented in Material Studio software. The structure factor was calculated from the elemental pair distribution functions. Other parameters were the coherent scattering amplitudes, f_α, and a Debye-Waller type root-mean square displacement of atoms due to thermal vibration. The scattering amplitudes were taken as: $f_H = -3.74$, $f_O = 5.80$ and $f_C = 6.65$ fermi [37].The scattering curve, $I(Q)$, is related by a Fourier transform operation to the radial distribution function. The calculated spectrum exhibits good agreement for the first three peaks at $Q = 0.58$, 1.53 and 3.07 $Å^{-1}$ as illustrated in Fig. 5. These locations fit the experimentally observed peaks that occur at $Q =$ 0.6, 1.33 and 3.0 $Å^{-1}$ quite well [31, 38]. The difference between the prediction and experiment lies in the intensity and the shape of the signal especially after the third peak. The scattering results indicate reasonable agreement to some extent between the computed and the actual structure.

CONCLUSIONS

This work illustrates a multiscale molecular modeling technique to generate and equilibrate the amorphous polymeric materials. A system of PEO structure was investigated using a combination of lattice Monte Carlo simulation and EM technique to mapping and reverse-mapping procedure between fully atomistic and coarse-grained chains. The local interaction parameters of polymer segment derived from an ab initio quantum chemistry calculation give a more accurate description of the conformational energies for each rotational isomeric state of polymer chains. Equilibrated structure of the amorphous PEO bulk was easily generated by this fast simulation technique with a great reduction of CPU time. The equilibrated structure from MC was reverse-mapped to a fully atomistic structure. Chain dimension, conformational characteristics, structural and thermodynamic properties were determined. The calculated results were in good agreement with those obtained by experiment.

ACKNOWLEDGMENTS

The project was supported by the Synchrotron Light Research Institute (Public Organization) (2-2548/PS02) and Suranaree University of Technology. The author thanks the Computational Nanotechnology Consortium for permission to use Materials Studio software. Kindly thanks to Prof. Wayne Mattice, Prof. Rahmi Ozisik, Prof. Pemra Doruker and Prof. Guoqiang Xu who have collaborated with the author on 2*nnd* project during the past years.

REFERENCES

1. M. Kotelyanskii and D. N. Theodorou, *Simulation Methods for Polymers* (CRC Press, New York, 2004).
2. P. E. Rouse, J. Chem. Phys. **21**, 1272 (1953).
3. M. Doi and S. Edwards, *Theory of Polymer Dynamics* (Clarendon, Oxford, 1986).
4. P. G. de Gennes, J. Chem. Phys. **55**, 572 (1971).
5. J. Baschnagel, K. Binder, P. Doruker, et al., Adv. Polym. Sci. **152**, 41 (2000).
6. R. F. Rapold and W. L. Mattice, J. Chem. Soc., Faraday Trans. **91**, 2435 (1995).

7. J. Cho and W. L. Mattice, Macromolecules **30**, 637 (1997).
8. P. Doruker and W. L. Mattice, Macromolecules **30**, 5520 (1997).
9. P. Doruker and W. L. Mattice, Macromolecules **32**, 194 (1998).
10. J. H. Jang and W. L. Mattice, Macromolecules **33**, 1467 (2000).
11. V. Vao-soongnern, P. Doruker, and W. L. Mattice, Macromol. Theory Simul. **9**, 1 (2000).
12. V. Vao-soongnern and W. L. Mattice, Macromol. Theory Simul. **9**, 570 (2000).
13. T. C. Clancy and W. L. Mattice, J. Chem. Phys. **112**, 10049 (2000).
14. V. Vao-soongnern, R. Ozisik, and W. L. Mattice, Macromol. Theory Simul. **10**, 553 (2001).
15. T. C. Clancy, J. H. Jang, A. Dhinojwala, and W. L. Mattice, J. Phys. Chem. B **105**, 11493 (2001).
16. E. D. Akten and W. L. Mattice, Macromolecules **34**, 3389 (2001).
17. G. Xu and W. L. Mattice, J. Chem. Phys. **116**, 2277 (2002).
18. G. Xu, H. W. L. Lin, and W. L. Mattice, J. Chem. Phys. **119**, 6736 (2003).
19. C. A. Helfer, G. Xu, W. L. Mattice, and C. Pugh, Macromolecules **36**, 10071 (2003).
20. P. Choi and W. L. Mattice, J. Chem. Phys. **121**, 8647 (2004).
21. S. S. Rane and W. L. Mattice, Macromolecules **37**, 7056 (2004).
22. V. Vao-Soongnern, G. Xu, and W. L. Mattice, Macromol. Theory Simul. **13**, 539 (2004).
23. S. S. Rane and W. L. Mattice, Macromolecules **38**, 3708 (2005).
24. P. J. Dionne, R. Ozisik, and C. R. Picu, Macromolecules **38**, 9351 (2005).
25. P. J. Dionne, C. R. Picu, and R. Ozisik, Macromolecules **39**, 3089 (2006).
26. V. Vao-soongnern, J. Nanosci. Nanotechnol. **6**, 3977 (2006).
27. V. Vao-soongnern, Comput. Mater. Sci. 49 (Suppl. 4), S369 (2010).
28. P. J. Flory, *Statistical Mechanics of Chain Molecules* (Wiley-Interscience, New York, 1969).
29. J. E. Mark and P. J. Flory, J. Am. Chem. Soc. **87**, 1415 (1965).
30. A. Abe, H. Furuya, M. K. Mitra, and T. Hiejima, Comput. Theor. Polym. Sci. **8**, 253 (1998).
31. O. Bolodin, R. Douglas, G. D. Smith, et al., J. Phys. Chem. B **107**, 6813 (2003).
32. C. Chen, P. Depa, V. G. Sakai, et al., J. Chem. Phys. **124**, 234901 (2006).
33. A. Leach, *Molecular Modelling: Principles and Applications* (Pearson Education, Harlow, 2009).
34. N. Metropolis, A. W. Rosenbluth, M. N. Rosenbluth, et al., J. Chem. Phys. **21**, 1087 (1953).
35. M. J. Fernandez-Berridi, T. F. Otero, G. M. Guzman, and J. M. Elorza, Polymer **23**, 1361 (1982).
36. P. J. Ludovice, PhD Thesis (Massachusetts Inst. Technol., Cambridge, 1989).
37. J. P. Cotton, D. Decker, H. Benoit, et al., Macromolecules **7**, 863 (1974).
38. B. K. Annis, O. Bolodin, G. D. Smith, et al., J. Chem. Phys. **115**, 10998 (2001).